AIP | Journal of Applied Physics

Effect of Cr deficiency on physical properties of triangular-lattice antiferromagnets CuCr1−xO2 (0x0.10)

D. C. Ling, C. W. Chiang, Y. F. Wang, Y. J. Lee, and P. H. Yeh

Citation: J. Appl. Phys. **109**, 07D908 (2011); doi: 10.1063/1.3544498

View online: http://dx.doi.org/10.1063/1.3544498

View Table of Contents: http://jap.aip.org/resource/1/JAPIAU/v109/i7

Published by the American Institute of Physics.

Effect of Cr deficiency on physical properties of triangular-lattice antiferromagnets $CuCr_{1-x}O_2$ ($0 \leqq x \leqq 0.10$)

D. C. Ling,[a] C. W. Chiang, Y. F. Wang, Y. J. Lee, and P. H. Yeh
Department of Physics, Tamkang University, Tamsui 25137, Taiwan

(Presented 16 November 2010; received 1 October 2010; accepted 5 November 2010; published online 24 March 2011)

Structural, transport, and magnetoelectric (ME) properties of delafossite oxides $CuCr_{1-x}O_2$ with $0 \leqq x \leqq 0.10$ were extensively investigated. The Rietveld refinement shows that the Cu-O bond length decreases with increasing Cr deficiency, indicative of the presence of a mixed valence state of Cu^+/Cu^{2+} and an enhancement of the hybridization between Cu 3*d* and O 2*p* orbitals. As a result, it leads to a decrease of room-temperature resistivity by two orders of magnitude. The deduced effective moment for the Cr-deficient samples is larger than the one only taking into account the contribution from Cr^{3+} with $S = 3/2$. This demonstrates that Cu^{2+} is present in the Cr-deficient samples, giving rise to excess holes at the Cu site. Below $T_N(\mathrm{Cr}) \sim 24$ K, the magnetocapacitance $[\varepsilon(H)-\varepsilon(0)]/\varepsilon(0)$ exhibits a distinct field dependence and deviates from the square of magnetization M^2. These findings suggest that the ME coupling in $CuCr_{1-x}O_2$ with higher *x* is modulated by an increase of the spin fluctuations in the CrO_2 triangular lattice through the interplay between charge and spin degrees of freedom.
[doi:10.1063/1.3544498]

Recently, spiral-magnetism-induced multiferroics have been discovered in some triangular-lattice antiferromagnets.[1–3] Among them, the delafossite oxide $CuCrO_2$ shows ferroelectricity induced by proper-screw spiral magnetic structures with a magnetic propagation vector ***q*** normal to the spiral plane.[4] More interestingly, the coercive electric and magnetic fields for ferroelectric polarization reversal in $CuCrO_2$ can be fine tuned by using both the external magnetic and electric fields.[5] This intriguing ME effect makes $CuCrO_2$ a promising candidate for new spin-based device applications. From the viewpoint of thermoelectric performance, the cation substituted $CuCrO_2$ is also very useful. For example, $CuCr_{0.97}Mg_{0.03}O_2$ exhibits a dimensionless figure of merit $ZT = 0.045$ at 1100 K,[6] similar to other layered triangular-lattice systems such as γ-$Na_{0.7}CoO_2$.[7] It has been shown that the partial substitution of Cr^{3+} by cations with similar ionic size can tune the spin chirality and modulate antiferromagnetism and ferroelectricity in multiferroic $CuCr_{1-x}M_xO_2$ ($M = Mg^{2+}$, Ca^{2+}, Al^{3+}, Mn^{3+}, and Ni^{3+}).[8–11] In spite of numerous investigations, a comprehensive understanding of magnetic ground state of $CuCrO_2$ is still lacking. In this work, a magnetic randomness-free approach was made by introducing Cr deficiency in the CrO_2 triangular lattice to elucidate the ME coupling in $CuCrO_2$. It is found that the oxygen-mediated interplay between the frustrated local spin at the Cr sites and the Cr-deficiency-induced holes at the Cu sites gives rise to a decent ME tenability and has a significant impact on physical properties of $CuCr_{1-x}O_2$ with $0 \leqq x \leqq 0.10$.

The investigated samples were prepared by the standard solid-state reaction method. A stoichiometric mixture of Cu_2O and Cr_2O_3 was ground thoroughly and then calcined at 900 °C in air for 24 h. The reactants were pressed into pellets and sintered at 1100 °C in air for 24 h with several grinding procedures. The structure and phase purity of the samples were characterized by x-ray powder diffraction (XRD) patterns with Cu K_α radiation. High-resolution transmission electron microscopy (HRTEM) images were collected on a JEOL 2100F field emission gun electron microscope operating at 200 kV. Resistivity, magnetization, and thermoelectric power (TEP) measurements were performed in a 9-T QUANTUM DESIGN physical property measurement system (PPMS). A dielectric constant was probed by an *LCR* meter integrated with PPMS.

Figure 1(a) shows XRD patterns for $CuCr_{1-x}O_2$ with $0 \leqq x \leqq 0.10$. All Bragg peaks can be indexed to the delafossite structure, two-dimensional triangular lattice layers formed by Cr^{3+} and Cu^+ ions alternately stacked along the *c*-axis as illustrated in the upper left panel of Fig. 1(b), with space group $R\bar{3}m$. No evident impurity peaks were detected in samples investigated. The HRTEM images for $CuCrO_2$ and $CuCr_{0.90}O_2$ along the [100] zone axis are shown in the upper right panels of Fig. 1(b). Clear lattice fringes were observed with the interplanar spacing of 2.84(8) Å for $CuCrO_2$ and 2.83(3) Å for $CuCr_{0.90}O_2$, respectively. This further supports the fact that the investigated samples are single-phased compounds with good crystalline quality. As shown in Fig. 1(b), the Rietveld-refined Cu-O bond length decreases with increasing Cr deficiency, accompanied by a tiny contraction of the *a* (Cu-Cu bond length)- and *c*-axis lattice constants (not shown), which is indicative of the presence of a mixed valence state of Cu^+/Cu^{2+} and an enhancement of the hybridization between Cu 3*d* and O 2*p* orbitals.[6,12,13] Consequently, it results in an increase of hole carriers in the Cu sites and is expected to tune physical properties of $CuCr_{1-x}O_2$ in a subtle way.

[a]Author to whom correspondence should be addressed. Electronic mail: dcling@mail.tku.edu.tw.

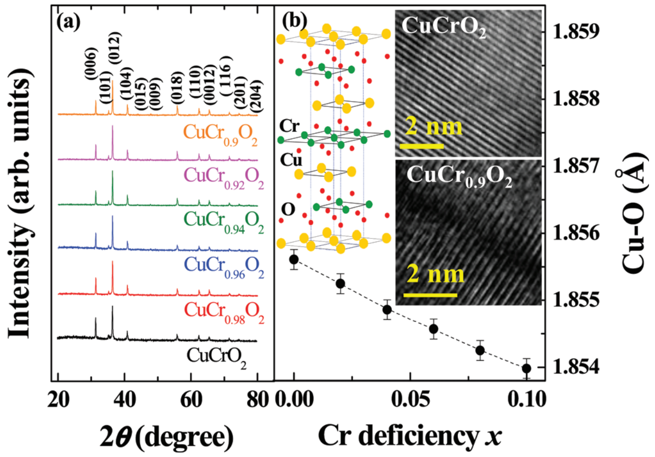

FIG. 1. (Color online) (a) XRD patterns for $CuCr_{1-x}O_2$ with $0 \leqq x \leqq 0.10$. (b) The Rietveld-refined Cu-O bond length as a function of Cr deficiency. The crystal structure of $CuCrO_2$ is shown in the upper left panel. The HRTEM images for $CuCrO_2$ and $CuCr_{0.90}O_2$ are displayed in the upper right panels.

The temperature dependence of the resistivity for the samples studied is displayed in Fig. 2. All samples exhibit an insulating behavior with $d\rho/dT < 0$ all the way down to low temperatures. It is remarkable that resistivity significantly decreases with increasing x within a wide temperature range. To quantitatively illustrate the Cr deficiency-dependent resistivity change, resistivity at 250 K ($\rho_{250\ K}$) as a function of x is plotted in the upper right panel of Fig. 2. Apparently, $\rho_{250\ K}$ decreases by more than two orders of magnitude with increasing x up to 0.08 from 6.82×10^5 Ω-cm for $CuCrO_2$ to 1.98×10^3 Ω-cm for $CuCr_{0.92}O_2$ and then slightly increases to 3.03×10^3 Ω-cm for $CuCr_{0.90}O_2$. This trend is qualitatively similar to what was reported for $CuCr_{1-x}Mg_xO_2$ with $0 < x < 0.04$,[12] indicating that holes are likely doped into the Cr-deficient samples. TEP as a function of temperature for samples studied with Seebeck coefficient α is presented in the lower right panel of Fig. 2. The positive sign of α confirms that the p-type carriers govern charge transport for the studied samples. In addition, α at 300 K increases with increasing x from 550 μV/K for $CuCrO_2$ to 990 μV/K

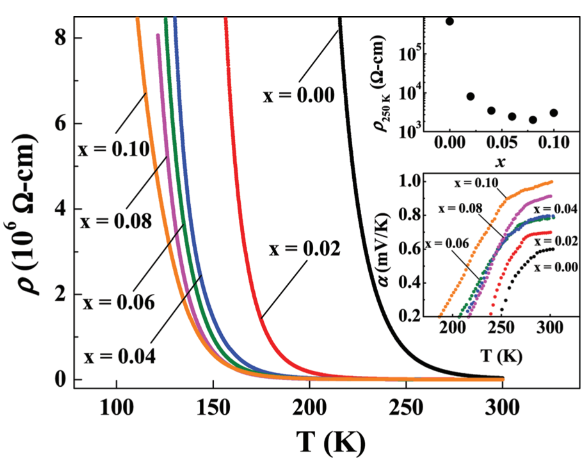

FIG. 2. (Color online) $\rho(T)$ for $CuCr_{1-x>}O_2$ with $0 \leqq x \leqq 0.10$. $\rho_{250\ K}(x)$ and $\alpha(T)$ for the studied samples are plotted in the upper and lower right panels, respectively.

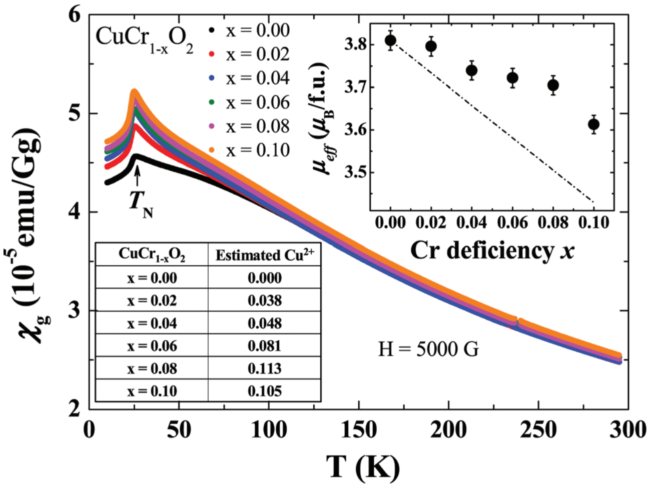

FIG. 3. (Color online) Zero-field-cooled $\chi(T)$ for the samples studied in a field of 5000 G. The deduced effective moment as a function of Cr deficiency is shown in the upper inset. A straight dashed line is the calculated μ_{eff}-x plot, assuming that the magnetic moment only contributes from Cr^{3+}. The estimated Cu^{2+} content is tabulated in the lower inset.

for $CuCr_{0.90}O_2$. Further investigation is needed to clarify the underlying origin of the extraordinarily high value of Cr-deficient-dependent α observed near room temperature.

To shed light on how the Cr deficiency modulates antiferromagnetic coupling between Cr ions in a geometrically frustrated lattice, the temperature dependence of the zero-field-cooled magnetic susceptibility for the samples studied in a field of 5000 G is illustrated in Fig. 3. An anomaly around 24 K, very robust against the Cr deficiency, is the Néel temperature T_N(Cr) associated with an out-of-plane 120° spin structure.[14] It is due to the fact that a tiny decrease of the a-axis lattice constant makes the change of the nearest-neighbor site spin-exchange interactions in the CrO_2 layers negligibly small. In the high-temperature regime of $T > 150$ K, the samples investigated are in a paramagnetic state and the corresponding magnetic data are well fitted by the Curie-Weiss law with expression of $\chi(T) = \chi_0 + \frac{C}{T+\theta}$, where χ_0 is a temperature-independent fitting parameter, C is the Curie constant, and θ is the Weiss constant. Note that θ is fitted to be about 180 K, 7.5 times larger than T_N, for the samples studied, indicative of substantial magnetic fluctuations in $CuCr_{1-x}O_2$ with $0 \leqq x \leqq 0.10$. The effective moment, $\mu_{eff} = \sqrt{3k_BC/N_A}$, is determined to be 3.81 ± 0.02 μ_B for $CuCrO_2$, which is quite close to the spin-only theoretical value of 3.87 μ_B for high spin Cr^{3+} with $S = 3/2$. The deduced effective moment as a function of Cr deficiency shown in the inset of Fig. 3 is found to decrease with increasing Cr deficiency. A straight dashed line sketched in the inset of Fig. 3 is the calculated μ_{eff}-x plot by assuming that the magnetic moment only contributes from Cr^{3+}. It is clear that the calculated μ_{eff} based upon the above assumption is smaller than the one deduced from magnetic measurements, regardless of x. This discrepancy is associated with the presence of Cu^{2+} ($3d^9$) with $S = 1/2$ for the Cr-deficient samples. In fact, it is self-consistently supported by a shrinking of the Cu-O bond length and the a-axis lattice constant for samples with higher x, as mentioned earlier. Provided that the spin-only $\mu_{eff}(Cu^{2+})$ is 1.73 μ_B, the amount of Cu^{2+}

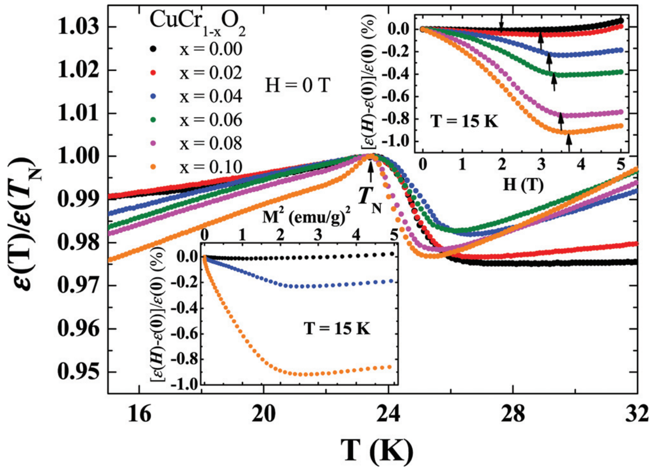

FIG. 4. (Color online) The normalized $\varepsilon(T)$ in zero field for samples studied in a temperature range from 15–32 K. Magnetocapacitance as a function of magnetic field at 15 K is shown in the upper inset. H^* is marked by an arrow. The lower inset displays the corresponding $[\varepsilon(H)-\varepsilon(0)]/\varepsilon(0)$ vs M^2 plot for samples with $x = 0.00$, 0.04, and 0.10.

(denoted as y) for the Cr-deficient samples can be estimated by the expression of $\mu_{eff,exp} = 3.81 \times (1-x) + 1.73 \times y$, where $\mu_{eff,exp}$ is the effective moment deduced from magnetic measurements. As tabulated in the inset of Fig. 3, the estimated Cu^{2+} content remarkably exhibits an opposite Cr deficiency dependence compared to $\rho_{250\ K}$. This strongly suggests that the excess holes doped into the Cu sites by the Cr deficiency are responsible for a decrease in resistivity of the Cr-deficient samples.

As shown in Fig. 4, the normalized dielectric constant as a function of temperature for $CuCr_{1-x}O_2$ with $0 \leqq x \leqq 0.10$ in zero field reveals a sharp anomaly at T_N(Cr), in good agreement with reported results,[1] indicative of a pronounced ME coupling between charge and spin degrees of freedom. To elucidate the ME effect and have a better understanding of the nature of the magnetic ground state, the magnetic field dependence of the magnetocapacitance $[\varepsilon(H-\varepsilon(0)]/\varepsilon(0)$ for the samples studied at 15 K is displayed in the upper inset of Fig. 4. Interestingly, magnetocapacitance decreases with increasing field up to H^* marked by an arrow and then slightly increases with increasing field up to 5 T. It has been shown that the field dependence of the $[\varepsilon(H)-\varepsilon(0)]/\varepsilon(0)$ is proportional to $\langle S_i \cdot S_j \rangle_H$ within a phenomenological model,[15] where $\langle S_i \cdot S_j \rangle_H$ is the spin-pair correlation of neighboring Cr spins at magnetic field H. In the mean-field approximation, if the magnetic fluctuation is negligible, $\langle S_i \cdot S_j \rangle_H = |\langle S| \rangle^2 \propto M^2$ where M is magnetization. It is expected that the sign of $\langle S_i \cdot S_j \rangle_H$ changes from negative to positive as H gradually increases from zero to H^* above which spins in an antiferromagnet are flipped into a ferromagnetic alignment. This scenario can account for the feature described above. In addition, the characteristic field H^* increases with increasing x from 1.96 T for $CuCrO_2$ to 3.71 T for $CuCr_{0.90}O_2$ and the magnitude of $[\varepsilon(H)-\varepsilon(0)]/\varepsilon(0)$ at $H < H^*$ monotonically increases with increasing x. It is most likely attributed to an enhancement of spin fluctuations arising from the coupling between the localized spins at the Cr sites and the itinerant Cr deficiency-induced holes at the Cu sites. This speculation is convincingly supported by the fact that $[\varepsilon(H)-\varepsilon(0)]/\varepsilon(0)$ is not simply proportional to the square of magnetization M^2 as shown in the lower inset of Fig. 4.

In summary, we have demonstrated that Cu^{2+} is induced, giving rise to excess holes at the Cu site, by the Cr deficiency in $CuCr_{1-x}O_2$ samples. Consequently, it leads to a significant decrease of room-temperature resistivity down to $\sim 10^3$ Ω-cm and a remarkable increase of Seebeck coefficient up to $\sim$1 mV/K for $CuCr_{0.90}O_2$. More importantly, the magnetocapacitance exhibits distinct features below T_N(Cr), suggesting that the ME coupling is modulated by an increase of spin fluctuations in $CuCr_{1-x}O_2$ with higher Cr deficiency through the interplay between charge and spin degrees of freedom.

This work was financially supported in part by the National Science Council of ROC under Grant No. NSC 96-2112-M-032-008-MY3.

[1] S. Seki, Y. Onose, and Y. Tokura, Phys. Rev. Lett. **101**, 067204 (2008).
[2] M. Kenzelmann, G. Lawes, A. B. Harris, G. Gasparovic, C. Broholm, A. P. Ramirez, G. A. Jorge, M. Jaime, S. Park, Q. Huang, A. Ya. Shapiro, and L. A. Demianets, Phys. Rev. Lett. **98**, 267205 (2007).
[3] T. Kimura, J. C. Lashley, and A. P. Ramirez, Phys. Rev. B. **73**, 220401(R) (2006).
[4] M. Soda, K. Kimura, T. Kimura, M. Matsuura, and K. Hirota, J. Phys. Soc. Jpn. **78**, 124703 (2009).
[5] K. Kimura, H. Nakamura, S. Kimura, M. Hagiwara, and T. Kimura, Phys. Rev. Lett. **103**, 107201 (2009).
[6] K. Hayashi, K. Sato, T. Nozaki, and T. Kajitani, Jpn. J. Appl. Phys. **47**, 59 (2008).
[7] L. Terasaki, Y. Sasago, and K. Uchinokura, Phys. Rev. B. **56**, R12685 (1997).
[8] T. Okuda, Y. Beppu, Y. Fujii, T. Onoe, N. Terada, and S. Miyasaka, Phys. Rev. B **77**, 134423 (2008).
[9] S. Luo, K. F. Wang, S. Z. Li, X. W. Dong, Z. B. Yan, H. L. Cai, and J.-M. Liu, Appl. Phys. Lett. **94**, 172504 (2009).
[10] A. Maignan, C. Martin, R. Frésard, V. Eyert, E. Guilmeau, S. Hébert, M. Poienar, and D. Pelloquin, Solid State Commun. **149**, 962 (2009).
[11] D. Li, X. Fang, W. Dong, Z. Deng, R. Tao, S. Zhou, J. Wang, T. Wang, Y. Zhao, and X. Zhu, J. Phys. D: Appl. Phys. **42**, 055009 (2009).
[12] T. Okuda, N. Jufuku, S. Hidaka, and N. Terada Phys. Rev. B **72**, 144403 (2005).
[13] R. Nagarajan, A. D. Draeseke, A. W. Sleight, and J. Tate, J. Appl. Phys. **89**, 8022 (2001).
[14] H. Kadowaki, H. Kikuchi, and Y. Ajiro, J. Phys.: Condens. Mater. **2**, 4485 (1990).
[15] T. Katsufuji and H. Takagi, Phys. Rev. B. **69**, 064422 (2004).